



1 **Technical note: 3-hourly temporal downscaling of monthly global**
2 **terrestrial biosphere model net ecosystem exchange**

3

4 Joshua B. Fisher^{1,*}, Munish Sikka¹, Deborah N. Huntzinger², Christopher
5 Schwalm³, Junjie Liu¹

6

7 ¹ Jet Propulsion Laboratory, California Institute of Technology, 4800 Oak Grove Drive, Pasadena, CA, 91109, USA

8 ² School of Earth Sciences and Environmental Sustainability, Northern Arizona University, 527 S. Beaver St.,
9 Flagstaff, AZ, 86011-5694, USA

10 ³ Woods Hole Research Center, Falmouth, MA, 02540, USA

11 * *Corresponding author. E-mail: jbfisher@jpl.nasa.gov*

12

13 Author contributions: JBF, DNH, and CS formulated idea; JBF and MS designed research; MS performed research;
14 DNH and CS provided data; all authors contributed to the writing of the paper.

15

16 The authors declare no conflict of interest.

17

18 Running title: 3-hourly temporal downscaling of monthly NEE



19 **Abstract**

20 The land surface provides a boundary condition to atmospheric forward and flux inversion
21 models. These models require prior estimates of CO₂ fluxes at relatively high temporal
22 resolutions (e.g., 3-hourly) because of the high frequency of atmospheric mixing and wind
23 heterogeneity. However, land surface model CO₂ fluxes are often provided at monthly time steps,
24 typically because the land surface modeling community focuses more on time steps associated
25 with plant phenology (e.g., seasonal) than on sub-daily phenomena. Here, we describe a new
26 dataset created from 15 global land surface models and 4 ensemble products in the Multi-scale
27 Synthesis and Terrestrial Model Intercomparison Project (MsTMIP), temporally downscaled
28 from monthly to 3-hourly output. We provide 3-hourly output for each individual model over 7
29 years (2004-2010), as well as an ensemble mean, a weighted ensemble mean, and the multi-
30 model standard deviation. Output is provided in three different spatial resolutions for user
31 preferences: 0.5° x 0.5°, 2.0° x 2.5°, and 4.0° x 5.0° (latitude/longitude). These data are publicly
32 available from: ftp://daac.ornl.gov/data/cms/CMS_NEE_CO2_Fluxes_TBMO/data.

33

34 *Keywords: CO₂ flux; downscale; land surface; NEE; sub-daily; hourly*



35 This technical note describes the methodological approach employed with temporally
 36 downscaling monthly terrestrial biosphere model (TBM) net ecosystem exchange (*NEE*) (i.e., net
 37 CO₂ flux between the land and atmosphere) output to 3-hourly time steps (Fisher et al., 2014).
 38 These data were created initially for NASA's Carbon Monitoring System (CMS), and are useful
 39 to the broader scientific community (Fisher et al., 2011; Fisher et al., 2012). The general
 40 downscaling approach follows Olsen and Randerson (2004) with modifications. The logic takes
 41 the components of *NEE*, i.e., gross primary production (*GPP*) and ecosystem respiration (*Re*),
 42 and links them with incident shortwave solar radiation (*I*) and surface air temperature (*T_a*),
 43 respectively. *I* and *T_a* are provided at 6-hourly time steps from CRU-NCEP (Wei et al., 2014a;
 44 Wei et al., 2014b), which we interpolated to 3-hourly time steps following cosines of solar zenith
 45 angle for *I* and linear interpolation for *T_a*. Hence, *GPP* and *Re* are temporally downscaled to 3-
 46 hourly, and re-combined to form *NEE* at 3-hourly time steps.

47
 48 The 6-hourly to two 3-hourly time steps from the solar zenith angle cosine interpolation follows
 49 this equation:

$$I_{t1} = \frac{I_t \times \cos z_{t1}}{\left(\frac{\cos z_{t1} + \cos z_{t-t1}}{2}\right)}, I_{t-t1} = \frac{I_t \times \cos z_{t-t1}}{\left(\frac{\cos z_{t1} + \cos z_{t-t1}}{2}\right)} \quad (1)$$

50 where *z* is solar zenith angle and *I_t* is in units of W m⁻². As an example, if the 0-6 hour *I_t* was 100
 51 W m⁻², and the 0-3 hour *z_{t1}* was 0 (i.e., cos(*z_{t1}*) = 1) and the 4-6 hour *z_{t-t1}* was 60 (i.e., cos(*z_{t-t1}*) =
 52 0.5), then the 0-3 hour *I_{t1}* would be 133.3 W m⁻², and the 4-6 hour *I_{t-t1}* would be 66.7 W m⁻².

53
 54 To scale *GPP* and *Re* to 3-hourly time steps, we followed Olsen and Randerson (2004) with
 55 modifications starting first with the calculation of scale factors based on *I* and *T_a*:

$$Q10_{3hr} = 1.5^{\frac{T_{a,3hr} - 30}{10}} \quad (2a)$$

$$T_{scale} = Q10_{3hr} / \sum_{30day} Q10_{3hr} \quad (2b)$$

$$I_{scale} = I_{3hr} / \sum_{30day} I_{3hr} \quad (3)$$

56 where *Q10* is the temperature dependency of *Re*, and *T_a* is in degrees Celsius (converted from
 57 Kelvin, as provided by CRU-NCEP). Note that Olsen and Randerson (2004) originally used time
 58 integral periods of calendar months, but we observed that this caused unrealistic distinct shifts
 59 between months. Instead, we modified the integral period to a 30-day moving window (Figure 1).
 60 For the first 15 days of January of the record and the last 15 days of December of the record, we
 61 used the last 15 days of December and the first 15 days of January, respectively, within the first
 62 (2004) and last (2010) years to complete the 30-day window.

63
 64 The 3-hourly resolution scale factors are then multiplied by *GPP* and *Re*, respectively, for each
 65 3-hourly time step each month:

$$Re_{3hr} = T_{scale} \times Re_{month} \quad (4)$$

$$GPP_{3hr} = I_{scale} \times GPP_{month} \quad (5)$$

66 We modified *Re_{month}* and *GPP_{month}* from Olsen and Randerson (2004) to be given at a 3-hourly
 67 time step, linearly interpolated to 3-hourly time steps based on the present, previous, and
 68 subsequent month, maintaining the original units (g C m⁻² mo⁻¹). *Re_{3hr}* and *GPP_{3hr}* are in units of
 69 g C m⁻² 3hr⁻¹. This modification avoided using the same monthly value for the multiplier for all
 70 3-hourly time steps per month as per Olsen and Randerson (2004), and instead provided a



71 smooth transition from one month to the next. The result of this modification was to eliminate a
 72 “ramping” effect whereby values would, for example, increase steadily within a month, then
 73 suddenly shift to a new starting point at the beginning of the next month (Figure 1). Note that the
 74 original nomenclature of Olsen and Randerson (2004) used $[(2 \times NPP_{month}) - NEP_{month}]$ in
 75 place of Re_{month} , and $(2 \times NPP_{month})$ in place of GPP_{month} , where NPP is net primary production
 76 (GPP minus autotrophic respiration) and NEP is net ecosystem production (approximately
 77 equivalent to the inverse sign of NEE , with caveats (Hayes and Turner, 2012)). The assumption
 78 here, therefore, is that $GPP = 2 \times NPP$ and $Re = (2 \times NPP) - NEP$. The Re assumption misses
 79 CO_2 emissions other than respiration, e.g., fire, which we correct for at a later step.

80

81 The initial NEE calculation simply subtracts GPP from Re :

$$NEE_{3hr} = Re_{3hr} - GPP_{3hr} \quad (4)$$

82 where NEE_{3hr} is calculated in units of $g\ C\ m^{-2}\ 3hr^{-1}$. However, we applied an additional units
 83 conversion for the publicly available data to $kg\ C\ km^{-2}\ s^{-1}$, as these units are more readily
 84 ingestible by atmospheric inversion models (Deng et al., 2014).

85

86 Because the downscaling approach uses Re as the primary CO_2 efflux term, other ecosystem CO_2
 87 loss components, such as fire and other disturbances (Hayes and Turner, 2012), are excluded in
 88 the downscale. Hence, the sum of the downscaled 3-hourly NEE fluxes in a given month did not
 89 necessarily equal the original monthly NEE flux. So, we included a per-pixel correction whereby
 90 we: I) calculated the difference between the sum of the downscaled 3-hourly NEE in a given
 91 month and the original monthly NEE ; II) divided that difference by the total 3-hourly time steps
 92 in the month, and III) added that difference to each 3-hourly NEE flux. In so doing, the sum of
 93 the downscaled 3-hourly NEE fluxes subsequently summed exactly to the original monthly NEE .

94

95 All input data were given in a spatial resolution of $0.5^\circ \times 0.5^\circ$ (latitude/longitude); hence, we
 96 provide the 3-hourly NEE output in $0.5^\circ \times 0.5^\circ$ (Figure 2). We also provide two additional sets of
 97 spatially upscaled NEE output in $2.0^\circ \times 2.5^\circ$ and $4.0^\circ \times 5.0^\circ$. These resolutions are used by the
 98 atmospheric modeling community, i.e., the GEOS-Chem atmospheric CO_2 transport model in the
 99 NASA CMS (Liu et al., 2014). To generate the coarser resolution data we: I) multiplied each
 100 pixel value by the land area of that pixel; II) summed the flux from all pixels that represent one
 101 pixel in coarser resolution (e.g., 8×10 pixels from $0.5^\circ \times 0.5^\circ$ comprise 1 pixel in $4.0^\circ \times 5.0^\circ$);
 102 III) calculated the total area covered by the pixels summed in step II; and, IV) divided the value
 103 in step II by the value in step III. The regridding preserved the total sum flux of the finer grid
 104 cells as well as the total global flux. We provide a file containing the land area contained in each
 105 latitudinal band for each of the 3 resolutions (folder name: ‘latitude_area’). We provide two
 106 versions of the $2.0^\circ \times 2.5^\circ$ and $4.0^\circ \times 5.0^\circ$ resolution products—one version with consistent
 107 global resolution, and another that conforms to the GEOS-Chem setup whereby the northern and
 108 southern most latitudinal bands for the $2.0^\circ \times 2.5^\circ$ resolution are $1.0^\circ \times 2.5^\circ$, and for the $4.0^\circ \times$
 109 5.0° they are $2.0^\circ \times 5.0^\circ$. The orientation of the global grid in the NetCDF files is transposed (i.e.,
 110 $90^\circ S \times 180^\circ W$ at top-left). The time vector represents the mid-point of each 3-hourly period.

111

112 Processing time in R, un-parallelized, on a standard PC for a single year for the forcing data was
 113 as follows:

- 114 • Interpolation of 6-hourly I and T_a to 3-hourly time step: 1 hr per variable
- 115 • 30-day moving window for I : 48 hr



- 116 • 30-day moving window for T_a : 68 hr
 117 • Total time to process forcing data for 7 years: $7*(1*2+48+68) = 826$ hr
 118

119 Processing time for the application of the modified Olsen and Randerson (2004) downscaling
 120 approach for a single model for a single year was:

- 121 • Monthly interpolation to 3-hourly time steps for GPP : 1 hr
 122 • Monthly interpolation to 3-hourly time steps for Re : 1 hr
 123 • GPP and Re downscaling: 2 hr
 124 • Monthly NEE closure correction: 1 hr
 125 • NetCDF generation with additional spatial resolutions: 2 hr
 126 • Total time to process all 19 products for 7 years: $7*19*(1+1+2+1+2) = 931$ hr
 127

128 The total storage size of the final NetCDF data products for all 19 products (15 models + 4
 129 ensemble products) for all 7 years is: 374 GB at $0.5^\circ \times 0.5^\circ$, 38 GB at $2.0^\circ \times 2.5^\circ$, and 10 GB at
 130 $4.0^\circ \times 5.0^\circ$.
 131

132 We provide the data in NetCDF with a separate file for each day per product at
 133 ftp://daac.ornl.gov/data/cms/CMS_NEE_CO2_Fluxes_TBMO/data. Each file contains the global
 134 gridded data with the eight 3-hourly intervals in the day. Open water pixels are set to 0, as this
 135 was desired by the atmospheric modeling community. However, we realize that NEE values can
 136 conceivably be 0 (though unlikely as our precision is to 16 decimal places); nonetheless, there
 137 are some pixels over land that are calculated as 0, but this is due to missing forcing data (e.g., I in
 138 the high latitudes during winter). Our code is set up that we can easily provide a different file
 139 output structure and missing value mask by request (contact the corresponding author:
 140 jbfisher@jpl.nasa.gov).
 141

142 Model output (GPP , Re , and NEE) was from the Multi-scale Synthesis and Terrestrial Model
 143 Intercomparison Project (MsTMIP) (Huntzinger et al., 2013; Huntzinger et al., 2016), version 1.
 144 15 models were included: 1) BIOME_BGC, 2) CLM, 3) CLM4VIC, 4) CLASS_CTEM, 5)
 145 DLEM, 6) GTEC, 7) ISAM, 8) LPJ-wsl, 9) ORCHIDEE, 10) SIB3, 11) SIBCASA, 12) TEM6,
 146 13) TRIPLEX-GHG, 14) VEGAS2.1, and 15) VISIT (Table 1). Additionally, 4 ensemble
 147 products were included: 1) un-weighted (naïve) ensemble mean, 2) un-weighted (naïve)
 148 ensemble standard deviation, 3) weighted (optimal) ensemble mean, and 4) weighted (optimal)
 149 ensemble standard deviation. Weights for model ensemble integration were derived based on
 150 model skill in reproducing GPP and biomass (Schwalm et al., 2015). Model output was obtained
 151 from: <ftp://nacp.ornl.gov/synthesis/2009/reutlingen/CMS/20141006/>
 152

153 To test and confirm the accuracy of our downscaling approach, we applied our method on a set
 154 of ground-truth data of measured NEE (and forcing variables) from the FLUXNET database
 155 (Baldocchi et al., 2001). We show, for example, a single year for a single site (3-hourly in
 156 background with daily-moving window overlaid) (Figure 3) and the scatterplot of calculated
 157 versus observed NEE values at the 3-hourly time step for that site and year (Figure 4). A full
 158 uncertainty analysis of the approach is beyond the scope of this technical note intended to
 159 describe the methodological detail of the downscaling.



160 **Acknowledgements**

161 Funding for this work was provided by NASA's Carbon Monitoring System (CMS) and NASA's
162 Carbon Cycle Science (CARBON) programs. We thank the MsTMIP modeling teams for
163 providing the model output. Access and information about MsTMIP model output can be found
164 at <http://nacp.ornl.gov/mstmipdata/>, along with model and model team participant information.
165 Funding for the MsTMIP activity was provided through NASA ROSES Grant
166 #NNX10AGO01A. Data management support for preparing, documenting, and distributing
167 MsTMIP model driver and output data was performed by the Modeling and Synthesis Thematic
168 Data Center at Oak Ridge National Laboratory with funding through NASA ROSES Grant
169 #NNH10AN681. We thank Dennis Baldocchi and Siyan Ma for providing the Tonzi Ranch
170 AmeriFlux/FLUXNET data; funding for AmeriFlux data resources and core site data was
171 provided by the U.S. Department of Energy's Office of Science. The research was carried out at
172 the Jet Propulsion Laboratory, California Institute of Technology, under a contract with the
173 National Aeronautics and Space Administration. Government sponsorship acknowledged.
174 Copyright 2016. All rights reserved.

175 **References**

- 176 Baker, I. T., Prihodko, L., Denning, A. S., Goulden, M., Miller, S., and da Rocha, H. R.:
177 Seasonal drought stress in the Amazon: Reconciling models and observations, *J. Geophys. Res.*,
178 113, G00B01, 2008.
- 179
- 180 Baldocchi, D., Falge, E., Gu, L. H., Olson, R. J., Hollinger, D., Running, S. W., Anthoni, P. M.,
181 Bernhofer, C., Davis, K., Evans, R., Fuentes, J., Goldstein, A., Katul, G., Law, B. E., Lee, X. H.,
182 Malhi, Y., Meyers, T., Munger, W., Oechel, W., U, K. T. P., Pilegaard, K., Schmid, H. P.,
183 Valentini, R., Verma, S., Vesala, T., Wilson, K., and Wofsy, S. C.: FLUXNET: A new tool to
184 study the temporal and spatial variability of ecosystem-scale carbon dioxide, water vapor, and
185 energy flux densities, *Bulletin of the American Meteorological Society*, 82, 2415-2434, 2001.
- 186
- 187 Baldocchi, D. and Ma, S.: How will land use affect air temperature in the surface boundary
188 layer? Lessons learned from a comparative study on the energy balance of an oak savanna and
189 annual grassland in California, USA, *Tellus B*, 65, 2013.
- 190
- 191 Deng, F., Jones, D., Henze, D., Bousserez, N., Bowman, K., Fisher, J., Nassar, R., O'Dell, C.,
192 Wunch, D., and Wennberg, P.: Inferring regional sources and sinks of atmospheric CO₂ from
193 GOSAT XCO₂ data, *Atmospheric Chemistry and Physics*, 14, 3703-3727, 2014.
- 194
- 195 Fisher, J. B., Huntzinger, D. N., Schwalm, C. R., and Sitch, S.: Modeling the terrestrial biosphere,
196 *Annual Review of Environment and Resources*, 39, 91-123, 2014.
- 197
- 198 Fisher, J. B., Polhamus, A., Bowman, K. W., Liu, J., Lee, M., Jung, M., Reichstein, M., Collatz,
199 G. J., and Potter, C.: Evaluation of NASA's Carbon Monitoring System Flux Pilot: terrestrial
200 CO₂ fluxes, San Francisco, CA2011.
- 201
- 202 Fisher, J. B., Sikka, M., Bowman, K. W., Liu, J., Lee, M., Collatz, G. J., Pawson, S., Gunson, M.,
203 CMS Flux Team, TRENDY Modelers, and NACP Regional Synthesis Modelers: The NASA
204 Carbon Monitoring System (CMS) Flux Pilot Project as a means to evaluate global land surface
205 models, American Geophysical Union Fall Meeting, San Francisco, 2012.
- 206
- 207 Hayes, D. and Turner, D.: The need for “apples - to - apples” comparisons of carbon dioxide
208 source and sink estimates, *Eos, Transactions American Geophysical Union*, 93, 404-405, 2012.
- 209
- 210 Hayes, D. J., McGuire, A. D., Kicklighter, D. W., Gurney, K. R., Burnside, T. J., and Melillo, J.
211 M.: Is the northern high-latitude land-based CO₂ sink weakening?, *Global Biogeochemical*
212 *Cycles*, 25, 2011.
- 213
- 214 Huang, S., Arain, M. A., Arora, V. K., Yuan, F., Brodeur, J., and Peichl, M.: Analysis of
215 nitrogen controls on carbon and water exchanges in a conifer forest using the CLASS-CTEM N+
216 model, *Ecological Modelling*, 222, 3743-3760, 2011.
- 217
- 218 Huntzinger, D., Schwalm, C., Michalak, A., Schaefer, K., King, A., Wei, Y., Jacobson, A., Liu,
219 S., Cook, R., Post, W., Berthier, G., Hayes, D., Huang, M., Ito, A., Lei, H., Lu, C., Mao, J., Peng,
220 C., Peng, S., Poulter, B., Ricciuto, D., Shi, X., Tian, H., Wang, W., Zeng, N., Zhao, F., and Zhu,



- 221 Q.: The North American Carbon Program Multi-scale synthesis and Terrestrial Model
222 Intercomparison Project–Part 1: Overview and experimental design, *Geoscientific Model*
223 *Development*, 6, 2121-2133, 2013.
224
- 225 Huntzinger, D. N., Schwalm, C. R., Wei, Y., Cook, R. B., Michalak, A. M., Schaefer, K.,
226 Jacobson, A. R., Arain, M. A., Ciais, P., Fisher, J. B., Hayes, D. J., Huang, M., Huang, S., Ito, A.,
227 Jain, A. K., Lei, H., Lu, C., Maignan, F., Mao, J., Parazoo, N., Peng, C., Peng, S., Poulter, B.,
228 Ricciuto, D. M., Tian, H., Shi, X., Wang, W., Zeng, N., Zhao, F., and Zhu, Q.: NACP MsTMIP:
229 Global 0.5-deg Terrestrial Biosphere Model Outputs (version 1) in Standard Format. DAAC, O.
230 (Ed.), Oak Ridge, Tennessee, USA, 2016.
231
- 232 Ito, A.: Changing ecophysiological processes and carbon budget in East Asian ecosystems under
233 near-future changes in climate: implications for long-term monitoring from a process-based
234 model, *Journal of plant research*, 123, 577-588, 2010.
235
- 236 Jain, A. K. and Yang, X.: Modeling the effects of two different land cover change data sets on
237 the carbon stocks of plants and soils in concert with CO₂ and climate change, *Global*
238 *Biogeochem. Cycles*, 19, GB2015, 2005.
239
- 240 Krinner, G., Viovy, N., de Noblet-DucoudrÈ, N., OgÈe, J., Polcher, J., Friedlingstein, P., Ciais,
241 P., Sitch, S., and Prentice, I. C.: A dynamic global vegetation model for studies of the coupled
242 atmosphere-biosphere system, *Global Biogeochem. Cycles*, 19, GB1015, 2005.
243
- 244 Li, H., Huang, M., Wigmosta, M. S., Ke, Y., Coleman, A. M., Leung, L. R., Wang, A., and
245 Ricciuto, D. M.: Evaluating runoff simulations from the Community Land Model 4.0 using
246 observations from flux towers and a mountainous watershed, *Journal of Geophysical Research:*
247 *Atmospheres*, 116, 2011.
248
- 249 Liu, J., Bowman, K. W., Lee, M., Henze, D. K., Bousserez, N., Brix, H., Collatz, G. J.,
250 Menemenlis, D., Ott, L., and Pawson, S.: Carbon monitoring system flux estimation and
251 attribution: impact of ACOS-GOSAT X CO₂ sampling on the inference of terrestrial biospheric
252 sources and sinks, *Tellus B*, 66, 2014.
253
- 254 Mao, J., Thornton, P. E., Shi, X., Zhao, M., and Post, W. M.: Remote Sensing Evaluation of
255 CLM4 GPP for the Period 2000-09*, *Journal of Climate*, 25, 5327-5342, 2012.
256
- 257 Olsen, S. C. and Randerson, J. T.: Differences between surface and column atmospheric CO₂
258 and implications for carbon cycle research, *Journal of Geophysical Research: Atmospheres*
259 (1984–2012), 109, 2004.
260
- 261 Peng, C., Liu, J., Dang, Q., Apps, M. J., and Jiang, H.: TRIPLEX: a generic hybrid model for
262 predicting forest growth and carbon and nitrogen dynamics, *Ecological Modelling*, 153, 109-130,
263 2002.
264

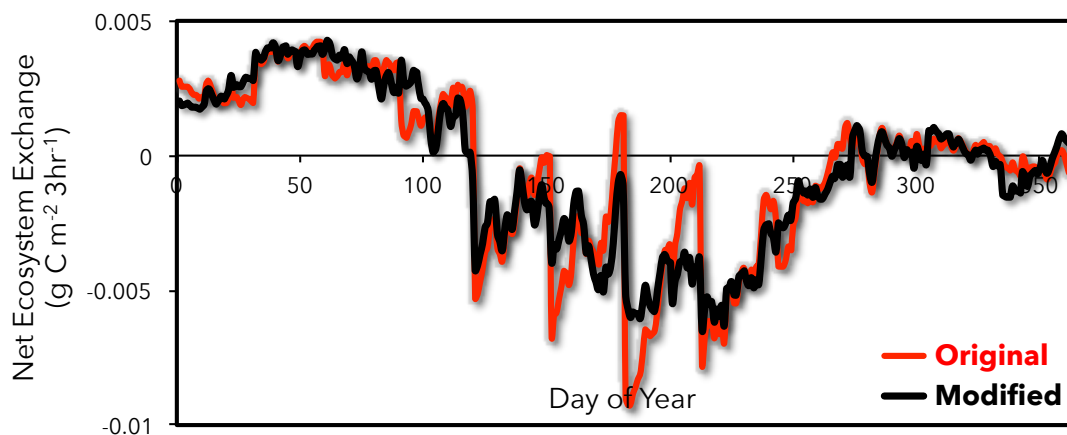


- 265 Ricciuto, D. M., King, A. W., Dragoni, D., and Post, W. M.: Parameter and prediction
266 uncertainty in an optimized terrestrial carbon cycle model: Effects of constraining variables and
267 data record length, *Journal of Geophysical Research: Biogeosciences* (2005–2012), 116, 2011.
268
- 269 Schaefer, K., Collatz, G. J., Tans, P., Denning, A. S., Baker, I., Berry, J., Prihodko, L., Suits, N.,
270 and Philpott, A.: Combined Simple Biosphere/Carnegie-Ames-Stanford Approach terrestrial
271 carbon cycle model, *Journal of Geophysical Research*, 113, G03034, 2008.
272
- 273 Schwalm, C. R., Huntzinger, D. N., Fisher, J. B., Michalak, A. M., Bowman, K., Ciais, P., Cook,
274 R., El - Masri, B., Hayes, D., and Huang, M.: Toward “optimal” integration of terrestrial
275 biosphere models, *Geophysical Research Letters*, 42, 4418-4428, 2015.
276
- 277 Sitch, S., Smith, B., Prentice, C. I., Arneth, A., Bondeau, A., Cramer, W., Kaplan, J. O., Lucht,
278 W., Sykes, M. T., Thonicke, K., and Venevsky, S.: Evaluation of ecosystem dynamics, plant
279 geography and terrestrial carbon cycling in the LPJ dynamic global vegetation model, *Global
280 Change Biology*, 9, 161-185, 2003.
281
- 282 Thornton, P. E., Law, B. E., Gholz, H. L., Clark, K. L., Falge, E., Ellsworth, D. S., Goldstein, A.
283 H., Monson, R. K., Hollinger, D., Paw U, J. C., and Sparks, J. P.: Modeling and measuring the
284 effects of disturbance history and climate on carbon and water budgets in evergreen needleleaf
285 forests, *Agricultural and Forest Meteorology*, 113, 185-222, 2002.
286
- 287 Tian, H., Chen, G., Zhang, C., Liu, M., Sun, G., Chappelka, A., Ren, W., Xu, X., Lu, C., and Pan,
288 S.: Century-scale responses of ecosystem carbon storage and flux to multiple environmental
289 changes in the southern United States, *Ecosystems*, 15, 674-694, 2012.
290
- 291 Wei, Y., Liu, S., Huntzinger, D., Michalak, A., Viovy, N., Post, W., Schwalm, C., Schaefer, K.,
292 Jacobson, A., and Lu, C.: NACP MsTMIP: Global and North American Driver Data for Multi-
293 Model Intercomparison. Data set. Available on-line [<http://daac.ornl.gov>] from Oak Ridge
294 National Laboratory Distributed Active Archive Center, Oak Ridge, Tennessee, USA. 2014a.
295
- 296 Wei, Y., Liu, S., Huntzinger, D., Michalak, A., Viovy, N., Post, W., Schwalm, C., Schaefer, K.,
297 Jacobson, A., and Lu, C.: The North American Carbon Program Multi-scale Synthesis and
298 Terrestrial Model Intercomparison Project–Part 2: Environmental driver data, *Geoscientific
299 Model Development*, 7, 2875-2893, 2014b.
300
- 301 Zeng, N., Qian, H., Roedenbeck, C., and Heimann, M.: Impact of 1998-2002 midlatitude drought
302 and warming on terrestrial ecosystem and the global carbon cycle, *Geophys. Res. Lett.*, 32,
303 L22709, 2005.
304
305

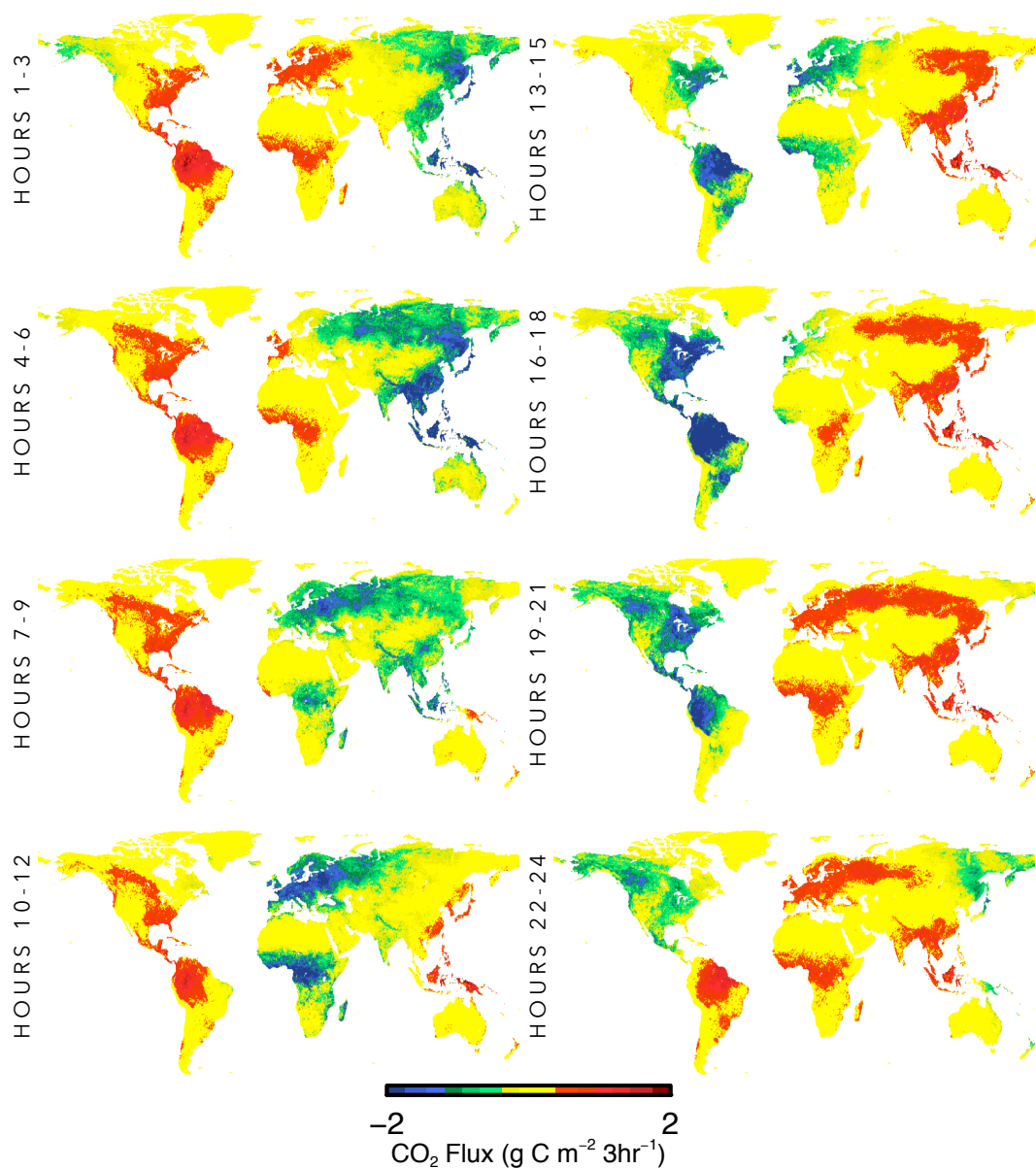


Model	Reference
BIOME_BGC	Thornton et al. (2002)
CLM	Mao et al. (2012)
CLM4VIC	Li et al. (2011)
CLASS_CTEM	Huang et al. (2011)
DLEM	Tian et al. (2012)
GTEC	Ricciuto et al. (2011)
ISAM	Jain and Yang (2005)
LPJ-wsl	Sitch et al. (2003)
ORCHIDEE	Krinner et al. (2005)
SIB3	Baker et al. (2008)
SIBCASA	Schaefer et al. (2008)
TEM6	Hayes et al. (2011)
TRIPLEX-GHG	Peng et al. (2002)
VEGAS2.1	Zeng et al. (2005)
VISIT	Ito (2010)

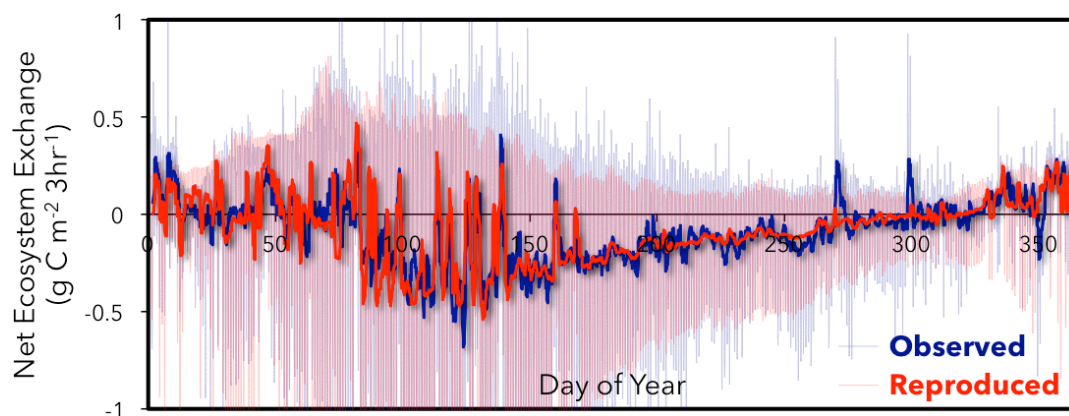
306 Table 1. Global terrestrial biosphere models from the Multi-scale Synthesis and Terrestrial
307 Model Intercomparison Project (MsTMIP) downscaled in this activity.



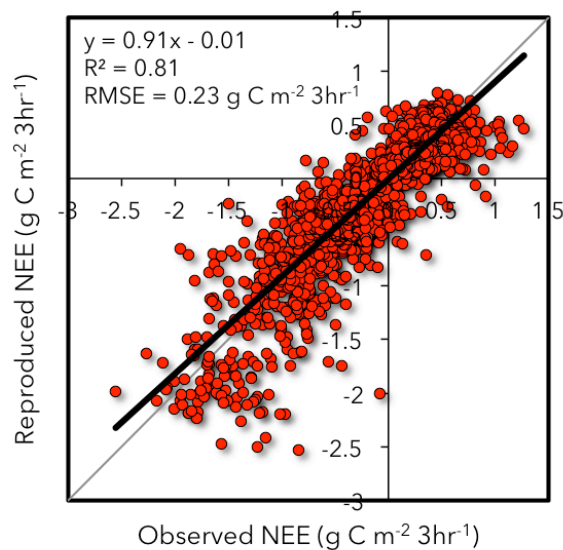
308
309 Figure 1. The original downscaling approach of Olsen and Randerson (2004) used monthly fixed
310 values, which led to a “stair-stepping” behavior between months (red). This was eliminated by
311 using a 30-day moving window and interpolating monthly input values to 3-hourly time steps
312 (black). Example shown for LPJ model global mean year 2005.



313 Figure 2. Vegetation productivity (e.g., blues/greens) follows the course of the sun for a single
314 day of net ecosystem exchange (NEE or net CO₂ flux; g C m⁻² 3hr⁻¹) for each 3-hourly period.
315 Shown here, for example, is July 1, 2007 for the weighted ensemble mean product.



316
317 Figure 3. The observed net ecosystem exchange (NEE) (blue) and reproduced NEE (red) shown
318 at the 3-hourly time step with daily moving window overlaid for a single year from the Tonzi
319 Ranch AmeriFlux/FLUXNET site (Baldocchi and Ma, 2013).



320
321 Figure 4. Observed versus reproduced net ecosystem exchange (NEE) at the 3-hourly time step
322 for a single year at the Tonzi Ranch AmeriFlux/FLUXNET site (Baldocchi and Ma, 2013).